

Leakage-Resistant Blood Vessels in Mice Transgenically Overexpressing Angiopoietin-1

G. Thurston,^{1*} C. Suri,² K. Smith,¹ J. McClain,² T. N. Sato,³
G. D. Yancopoulos,^{2*} D. M. McDonald¹

Angiopoietin-1 (Ang1) and vascular endothelial growth factor (VEGF) are endothelial cell-specific growth factors. Direct comparison of transgenic mice overexpressing these factors in the skin revealed that the VEGF-induced blood vessels were leaky, whereas those induced by Ang1 were nonleaky. Moreover, vessels in Ang1-overexpressing mice were resistant to leaks caused by inflammatory agents. Coexpression of Ang1 and VEGF had an additive effect on angiogenesis but resulted in leakage-resistant vessels typical of Ang1. Ang1 therefore may be useful for reducing microvascular leakage in diseases in which the leakage results from chronic inflammation or elevated VEGF and, in combination with VEGF, for promoting growth of nonleaky vessels.

Angiopoietin-1 (Ang1) and vascular endothelial growth factor/vascular permeability factor (VEGF) play separate but essential roles in vascular development during embryogenesis: VEGF acts early in development during formation of the initial vascular plexus, whereas Ang1 acts during the subsequent remodeling of the vasculature into a hierarchical network of mature vessels composed of endothelial and adventitial cells (1). Consistent with their putative roles in vascular development, Ang1 or VEGF overexpressed in mouse skin results in increased vascularity (2, 3). Dermal microvessels of mice overexpressing Ang1 (K14-Ang1 mice) are significantly larger than normal and the skin appears reddened (2). In comparison, dermal microvessels of mice overexpressing VEGF (K14-VEGF mice) are unusually numerous and show signs of inflammation, including increased adhesion of leukocytes (3). The ear skin of mice overexpressing VEGF is also thickened (3), which is consistent with the presence of tissue edema due to the permeability-increasing action of VEGF (4, 5).

To explore the possibility that the increased skin thickness in K14-VEGF mice (3) was due to the permeability-increasing actions of VEGF, we generated a similar line of mice (6). As with K14-Ang1 mice, the skin of K14-VEGF mice was redder than normal, but, unlike the skin of K14-Ang1 mice, it was also thicker than normal (Fig. 1), with regions of increased cellularity and foci of inflammatory cells. In addition, at 10 to 12

weeks of age, focal red skin lesions began to develop on the ears of the K14-VEGF mice (Fig. 1). These lesions were found to be hemorrhagic ulcers marked by extravasated red blood cells and disrupted epidermis. For subsequent studies, we focused on the vessels in ear skin (6).

We first compared the morphology of vessels in the ear skin of K14-VEGF and K14-Ang1 mice. The overall vascularity, as assessed by vessel area density, was increased in both K14-VEGF and K14-Ang1 mice. However, these increases resulted from distinctly different changes in the microvasculature. Overexpression of VEGF resulted in abundant small, tortuous vessels (Fig. 2, A and B), which resembled capillaries. In contrast, overexpression of Ang1 resulted in prominent enlargement of vessels, especially around hair follicles near the periphery of the ear (Fig. 2C). Although these vessels were in the anatomic position of capillaries, they resembled postcapillary venules (7). Measurements confirmed that the increase in vessel area density in K14-VEGF mice was primarily due to increases in vessel length, whereas in K14-Ang1 mice it was primarily due to increases in vessel diameter (8).

To determine whether the Ang1 phenotype or the VEGF phenotype was dominant, we bred K14-Ang1 and K14-VEGF mice to produce double transgenic K14-Ang1/VEGF mice. Vessels in the ear skin of K14-Ang1/VEGF mice were a composite of numerous tortuous capillary-like vessels (Fig. 2D), similar to those in mice overexpressing VEGF alone, and enlarged microvessels, similar to those in mice overexpressing Ang1 alone. The vessel area density in K14-Ang1/VEGF mice was greater than that in either K14-VEGF or K14-Ang1 mice (8). The increased vessel area density was due to an increase in length density and an increase in vessel di-

ameter. The combination of these two growth factors seemed to be additive in terms of vessel morphology and angiogenesis.

We next compared vascular leakiness in the transgenic mice under baseline conditions. We injected Evans blue dye into the femoral vein and measured leakage of dye from the vasculature. Ear skin vessels in K14-VEGF mice were abnormally leaky under baseline conditions (Fig. 3A, open bars). In comparison, skin vessels in K14-Ang1 mice were not leaky (Fig. 3A). Furthermore, baseline plasma leakage in double transgenic K14-Ang1/VEGF mice was significantly less than in K14-VEGF mice (Fig. 3A) and was in the range of that in wild-type mice. These findings show that coexpression of Ang1 can reduce vascular leakage due to overexpression of VEGF.

We investigated the response of these vessels to mustard oil, an inflammatory agent that induces plasma leakage and inflammation in the skin (9, 10). After injection of Evans blue and topical application of mustard oil, the ears of wild-type mice became moderately blue, particularly at the periphery (Fig. 3B). In contrast, the ears of K14-VEGF mice became uniformly blue (Fig. 3C). Strikingly, the ears of K14-Ang1 mice remained pale after treatment with mustard oil (Fig. 3D). Spectrophotometric analysis revealed that leakage increased sixfold in wild-type mice 30 min after application of mustard oil (Fig. 3A, closed bars). Leakage in K14-VEGF mice, already elevated under baseline conditions, increased further (Fig. 3A). However, leakage did not increase significantly in ear skin of K14-Ang1 mice and was significantly less than that in wild-type and K14-VEGF mice (Fig. 3A).

To determine whether the resistance to plasma leakage of K14-Ang1 mice was specific to mustard oil, we tested the responses to serotonin and platelet activating factor (PAF) (11) and found the vessels resistant to both (Fig. 3F) (12). Indeed, K14-Ang1 mice were also resistant to injection of the vehicle alone, which induced a slight increase in leakage in wild-type mice (Fig. 3F). Thus, transgenic overexpression of Ang1 gave rise to vessels that were resistant to leakage induced by inflammatory stimuli.

To address the question of whether the Ang1 phenotype or the VEGF phenotype was dominant in terms of inflammation-induced vessel leakiness, we also examined mustard oil-induced leakage in double transgenic K14-Ang1/VEGF mice. After treatment with mustard oil, plasma leakage in the double transgenic mice was significantly less than in K14-VEGF mice and was even less than that in wild-type mice (Fig. 3, A and E). These findings indicate that Ang1 can reduce vascular leakage due to inflammatory mediators even in the presence of excess VEGF.

¹Department of Anatomy and Cardiovascular Research Institute, University of California, San Francisco, CA 94143-0452, USA. ²Regeneron Pharmaceuticals Inc., Tarrytown, NY 10591, USA. ³University of Texas, Southwestern Medical Center, Dallas, TX 75235, USA.

*To whom correspondence should be addressed. E-mail: gavint@itsa.ucsf.edu or gdy@regpha.com

REPORTS

Fig. 1. Comparison of untreated ear skin of wild-type, K14-VEGF, and K14-Ang1 mice. (A to C) Untreated ears showing reddened ears of K14-VEGF and K14-Ang1 mice. (B, inset) Focal red lesions (arrow) in ear skin of older (>12 weeks) K14-VEGF mouse. The focal lesions appeared in single-copy K14-VEGF mice at about 16 weeks of age and in double-copy K14-VEGF mice at 8 to 10 weeks. (D to F) Thickened ear skin of K14-VEGF mouse and normal thickness of K14-Ang1 mouse shown in tissue sections of ear skin. Frozen sections of ear skin stained with antibodies to CD31 (platelet/endothelial cell adhesion molecule); purple, alkaline phosphatase reaction. Section through focal lesion of K14-VEGF mouse ear shows dense network of vessels and disruption of epidermis (E, inset). Ear skin of K14-Ang1 mouse (F) was normal thickness.

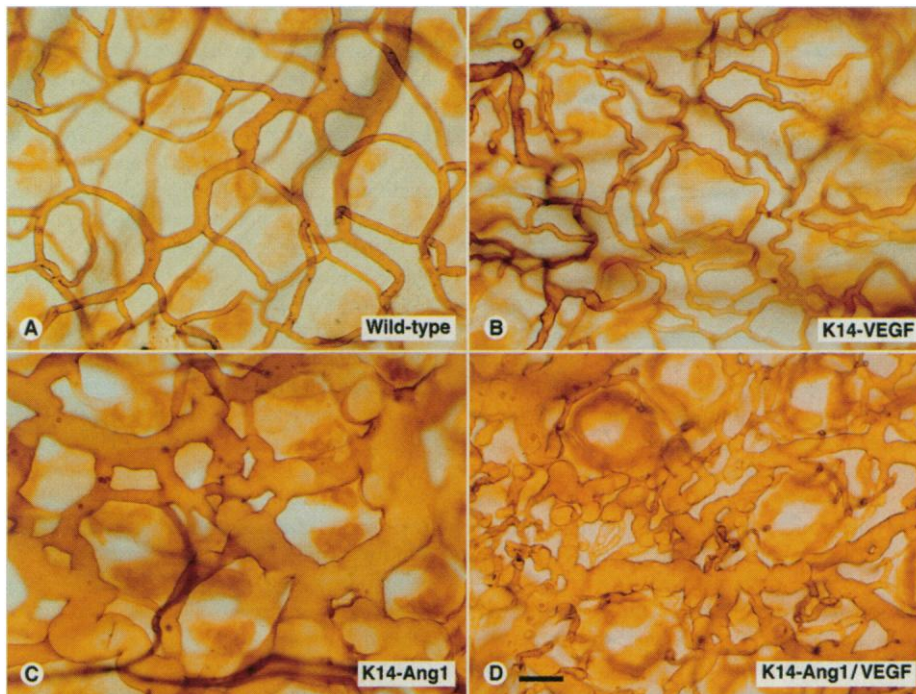
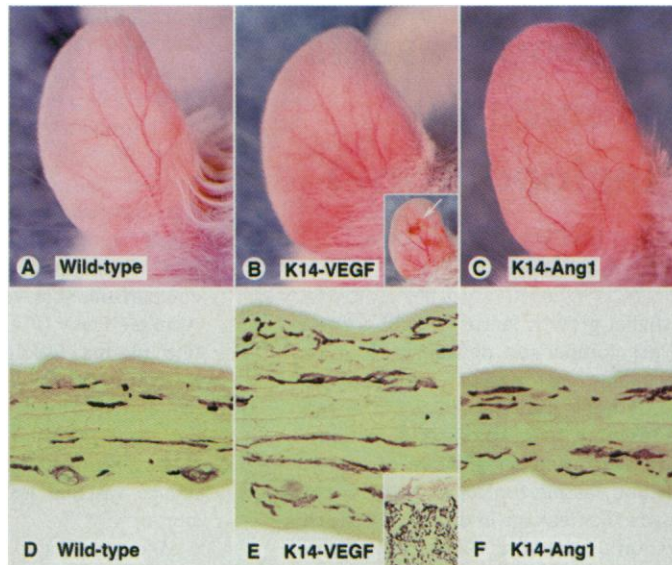


Fig. 2. (A to D) Comparison of microvessel morphology near margin of ear in lectin-stained whole mounts of ear skin. Vessels were stained by perfusion of biotinylated *Lycopersicon esculentum* lectin and visualized by ABC-3,3'-diaminobenzidine (DAB) peroxidase reaction (2, 26). Abundant tortuous, capillary-sized vessels in a K14-VEGF mouse contrast with large vessels in a K14-Ang1 mouse. Vessels in a double-transgenic K14-Ang1/VEGF mouse have features of both single transgenics: abundant tortuous vessels and some enlarged vessels. After perfusion fixation, mice were perfused with biotinylated *L. esculentum* lectin (25 ml at 5 μ g/ml) (Vector Laboratories, Burlingame, CA). *L. esculentum* lectin binds uniformly to the luminal surface of endothelial cells and adherent leukocytes (26). Ears were removed and the skin was separated from the cartilage. Ear skin whole mounts were permeabilized with 0.3% Triton X-100, incubated in avidin-peroxidase complex (Vector Laboratories) overnight, and reacted with 0.5% DAB (Sigma) and hydrogen peroxide. Ear skin was dehydrated through a series of alcohols, cleared in toluene, and mounted with the dermal aspect up. Scale bar = 25 μ m.

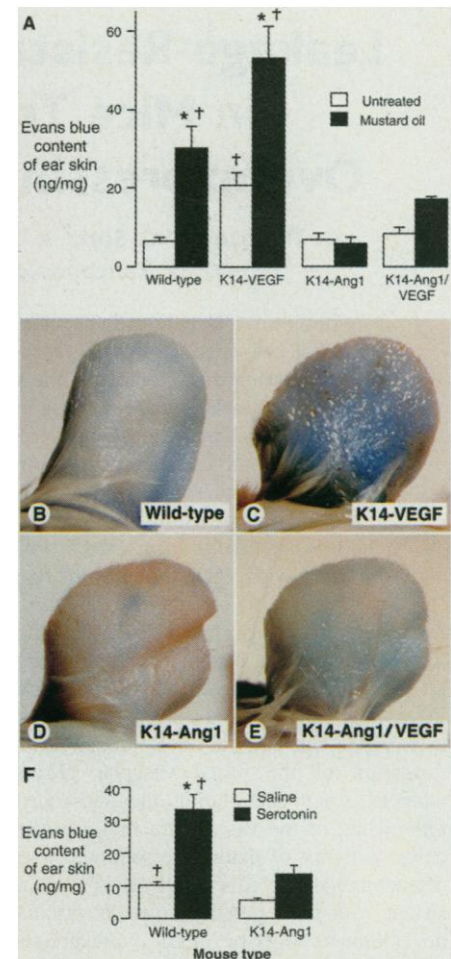


Fig. 3. Comparison of plasma leakage in ear skin after treatment with inflammatory agents. (A) Spectrophotometric measurement of amount of extravasated Evans blue (23, 27) in mouse ears 30 min after topical application of mustard oil. Baseline leakage (open bars) was elevated in K14-VEGF mice but not in K14-Ang1 or K14-Ang1/VEGF mice. Mustard oil treatment (closed bars) induced significant leakage in vessels of wild-type and K14-VEGF mice. However, no such increase was found in vessels of K14-Ang1 mice and there was only a moderate increase in K14-Ang1/VEGF mice. (B to E) Photographs of ears after treatment with mustard oil (30 min) and vascular perfusion, showing relative amount of extravasated Evans blue tracer. Ear from a wild-type mouse is blue around the margin of the ear, whereas ear from a K14-VEGF mouse is strongly blue throughout the ear. Ear from a K14-Ang1 mouse is almost white, and ear from a K14-Ang1/VEGF mouse is slightly blue. (F) Amount of extravasation of Evans blue in ears of wild-type and K14-Ang1 mice 30 min after intradermal injection of serotonin (closed bars). Again, there was less leakage in K14-Ang1 mice than in wild-type mice. Similar results were obtained with PAF (12). Evans blue (EM Sciences, Cherry Hill, NJ) (30 mg/kg in a volume of 100 μ l) was injected into a femoral vein of anesthetized mice. Values are mean \pm SEM; $n = 4$ to 6 mice per group. *Significantly greater leakage in treated ears than in corresponding untreated ears, $P < 0.05$. †Significantly greater leakage than in corresponding ears of K14-Ang1 mice. $P < 0.05$, Bonferroni-Dunn test.

REPORTS

The amount of plasma leakage in inflammation depends on the number and size of sites for leakage in the endothelium as well as the driving forces across the endothelium into the interstitium (13). Therefore, we asked whether the reduced leakage in K14-Ang1 mice was associated with reduced numbers of leakage sites in the endothelium. Because leakage sites expose the endothelial basement membrane to

the vessel lumen, we visualized these sites by staining the exposed basement membrane and extravascular matrix with biotinylated *Ricinus communis* I lectin perfused through the vasculature after fixation (14). In untreated vessels, ricin bound uniformly to the luminal surface of the endothelium (Fig. 4A). After treatment with mustard oil, ricin bound strongly to focal sites of exposed basement membrane in venules of wild-type mice (Fig. 4B). The lectin bound uniformly to the luminal surface of arterioles and capillaries without focal sites of binding, indicating that the sites of leakage were restricted to venules, as in other models of acute inflammation (15).

In K14-Ang1 mice, ricin bound weakly to all vessels under baseline conditions, but ricin also bound uniformly after treatment with mustard oil (Fig. 4D). Occasional sites of focal ricin binding in venules indicated that the lectin could detect sites of exposed basement membrane (Fig. 4D). Leakage sites were not found in arterioles or capillaries in K14-Ang1 mice, as in wild-type mice. These results suggest that the reduced plasma leakage in K14-Ang1 mice reflects a reduced number of leakage sites in venules and not hemodynamic changes.

In K14-VEGF mice, most capillaries and venules did not have focal leaks under baseline conditions, nor was leakage found in arterioles. However, occasional sites of ricin binding were found in some small venules and capillary-like vessels under baseline conditions (Fig. 4E). After stimulation with mustard oil, the large increase in leakage of Evans blue dye was accompanied by formation of numerous ricin binding sites of leakage in venules and capillaries (Fig. 4, C and F) but not in arterioles. This leakage from capillaries in K14-VEGF mice is unusual, because leakage was restricted to venules in wild-type mice. Previous studies have shown that direct application of VEGF can also induce leakage from capillaries (5).

Very few ricin binding sites were present in vessels of double transgenic K14-Ang1/VEGF mice under baseline conditions, and the number was moderately increased after treatment with mustard oil (16). Overexpression of Ang1 thus reduced the high baseline leakage as well as the inflammatory leakage associated with overexpression of VEGF, but it did not reduce the angiogenic effect of VEGF and instead appeared to act additively.

Our findings extend the evidence that VEGF and Ang1 play complementary and coordinated roles in vascular development and remodeling (1) and raise the possibility that these factors play an ongoing role in regulation of vascular permeability. Although the mechanisms by which VEGF and Ang1 produce their effects on vessel morphology and vessel leakiness are just beginning to be studied, they are presumably initiated by binding to their respective receptors on endothelial cells, the activa-

tion of endothelial cell signaling cascades, and subsequent endothelial cell-mediated remodeling of the microvessels.

Therapeutic angiogenesis, the induction of new vessel growth into ischemic tissue, has become an exciting direction of clinical research. Endothelial cell-specific growth factors have been used to promote angiogenesis in conditions of occlusive vascular disease. For example, administration of plasmid DNA encoding VEGF has been reported to promote new vessel growth and improved tissue perfusion in patients with ischemic limb (17) or heart disease (18). However, some patients treated with VEGF plasmid for lower limb ischemia may have transient limb edema (17, 19), possibly due to the permeability increasing effect of VEGF. Our study raises the possibility that a combination of VEGF and Ang1 could have additive effects in promoting angiogenesis plus the beneficial effect of forming nonleaky vessels. Importantly, the abundant angiogenesis in K14-Ang1/VEGF mice suggests that the angiogenic action of VEGF can be uncoupled from its leakage-inducing effects by Ang1.

Regulation of vascular permeability has clinical ramifications beyond the field of therapeutic angiogenesis. Plasma leakage and edema are features of inflammatory, degenerative, and neoplastic diseases. For example, chronic inflammatory diseases of the airways such as asthma are associated with edema in the airway wall and narrowing of the airway lumen (20), diabetic retinopathy is associated with plasma leakage in the retina (21), and ovarian cancers can be associated with massive fluid accumulation in the peritoneum (22). Plasma leakage is a key feature of the pathophysiology of these diseases, and inhibition of the leakage could have important therapeutic benefits. Ang1 has the potential to reduce plasma leakage in such conditions, whether the leak is due to inflammatory mediators or to VEGF.

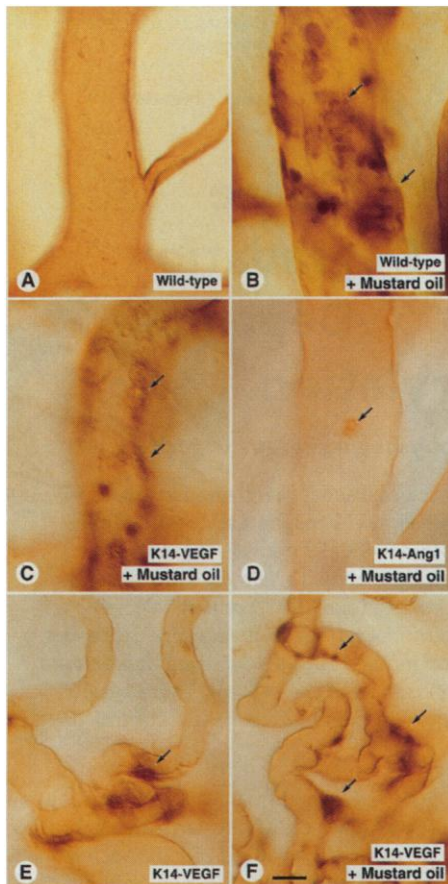


Fig. 4. Leakage sites in skin microvessels stained by perfusion of ricin lectin after topical application of mustard oil. At 20 min after mustard oil treatment, vessels were perfused with biotinylated ricin lectin and then stained with ABC-DAB peroxidase reaction mixture. Patches of dark ricin staining mark sites of binding to exposed basement membrane, which show vascular leaks (26). (A) Venule in untreated ear skin of wild-type mouse showing uniform ricin staining on endothelial cell surface. (B) Venule in mustard oil-treated ear skin of wild-type mouse with dark patches of ricin staining (arrows) indicating sites of exposed basement membrane. (C) Venule in mustard oil-treated ear skin of K14-VEGF mouse with dark patches of ricin staining (arrows). (D) Venule in mustard oil-treated skin of K14-Ang1 mouse with rare dark ricin patch (arrow). (E) Capillaries from untreated ear of K14-VEGF mouse showing focal patches of dark ricin staining (arrow) under baseline conditions. (F) Capillaries in mustard oil-treated ear skin of K14-VEGF mouse with numerous dark patches of ricin staining (arrows). Vasculature was stained by postfixation perfusion of *R. communis* I (ricin) lectin (Vector Laboratories) (26). Scale bar = 10 μ m.

References and Notes

1. D. Hanahan, *Science* **277**, 48 (1997); N. Ferrara and T. Davis-Smyth, *Endocr. Rev.* **18**, 4 (1997); N. W. Gale and G. D. Yancopoulos, *Genes Dev.* **13**, 1055 (1999); C. Suri et al., *Cell* **87**, 1171 (1996); J. Folkman and P. A. D'Amore, *Cell* **87**, 1153 (1996); P. C. Maisonpierre et al., *Science* **277**, 55 (1997).
2. C. Suri et al., *Science* **282**, 468 (1998).
3. M. Detmar et al., *J. Invest. Dermatol.* **111**, 1 (1998).
4. H. F. Dvorak et al., *Am. J. Pathol.* **146**, 1029 (1995).
5. W. G. Roberts and G. E. Palade, *J. Cell Sci.* **108**, 2369 (1995).
6. The keratin-14 promoter directs expression to the basal layer of the epidermis, including cells lining the hair follicles (2). To directly compare K14-Ang1 and K14-VEGF mice, we generated a line of K14-VEGF mice by an approach identical to that used for the K14-Ang1 mice (2), except cDNA encoding mouse VEGF₁₆₄ was used. This line of K14-VEGF mice was phenotypically similar to those generated by Detmar et al. (3). In a previous study we examined single-allele K14-Ang1 mice (2), whereas in this study we used double-allele K14-Ang1 mice. As previously reported, both transgenic strains of mice were fertile and overtly healthy (2, 3). The ear skin of both K14-VEGF and K14-Ang1 mice was redder than that of wild-type FVB/N mice. Otherwise the skin of

K14-Ang1 mice appeared normal, and histological sections revealed that the ear skin was similar to that of wild-type mice in terms of both thickness and cellular components; the only obvious difference in the K14-Ang1 skin was an increased number of large vessels. In contrast, the ear skin of K14-VEGF mice appeared thicker than normal (3), and by the time the mice were 10 to 12 weeks of age focal red skin lesions began to develop in their ears. We focused on the ear skin of mice because (i) the vasculature is not obscured by dense hair, (ii) the ear vasculature can easily be examined in whole mounts, (iii) the ears can easily be examined while the mice are alive, and (iv) the ear skin seemed to resemble the remainder of the skin. Different amounts of Ang1 or VEGF expression in different regions of skin, perhaps as a result of different density of hair follicles, could result in quantitative differences in vessel length and area density.

7. The phenotype of the ear microvessels was determined by examining the venule-specific endothelial cell markers P-selectin and von Willebrand factor (vWF) (23) and the pericyte marker desmin. In K14-Ang1 mice we found strong immunoreactivity for P-selectin and vWF in venules and in vessels in the anatomic position of capillaries, but in wild-type mice we found strong immunoreactivity for these markers only in venules. Further, the pericytes of these vessels in K14-Ang1 mice had the highly branched morphology of venules instead of the elongated morphology of capillaries.
8. The vessel length density in ear skin of K14-VEGF mice (63.5 ± 2.8 mm/mm²) was 56% greater than that in wild-type mice (40.7 ± 1.2 mm/mm²) and 37% greater than that in K14-Ang1 mice (46.3 ± 2.4 mm/mm²). In contrast, the average capillary diameter in K14-Ang1 mice (15.8 ± 0.8 μm) was 90% greater than that in wild-type mice (8.3 ± 0.6 μm) and 147% greater than that in K14-VEGF mice (6.4 ± 0.3). The vessel length density in K14-Ang1/VEGF mice was further increased (66.7 ± 3.9 mm/mm²), whereas the average capillary diameter was normal (8.7 ± 0.1 μm) due to averaging unusually large and small vessels. Supplementary material is available at www.sciencemag.org/feature/data/1043334.sml
9. H. Inoue et al., *Eur. J. Pharmacol.* **333**, 231 (1997).
10. An inflammatory agent, mustard oil or serotonin, known to cause plasma leakage in mouse skin (9, 24), was applied to the ear 1 min after injection of Evans blue dye. Mustard oil (Sigma) was diluted to 5% in mineral oil and applied to the dorsal and ventral surfaces of the ear with a cotton tip; it was reapplied 15 min later. Nothing was done to the other ear of mice treated with mustard oil (baseline control). Serotonin (Sigma) was dissolved at 0.22 mg/ml in sterile 0.9% NaCl plus 0.005 N acetic acid (vehicle). About 10 μl was injected (28G needle) intradermally into the dorsal ear skin, and a similar volume of vehicle was injected into the other ear (control). Thirty minutes after the stimulus, the vasculature was perfusion-fixed (1% paraformaldehyde in 50 mM citrate buffer, pH 3.5) for 2 min. Ears were removed, blotted dry, and weighed. Evans blue was extracted from the ears with 1 ml of formamide overnight at 55°C and measured spectrophotometrically at 610 nm.
11. E. Fujii et al., *Naunyn-Schmiedeberg Arch. Pharmacol.* **350**, 361 (1994).
12. Injection of PAF (80 μg/ml) in the ear skin of wild-type mice increased Evans blue content to 41.2 ± 10.0 ng/mg, whereas in K14-Ang1 mice the amount was 23.2 ± 4.1 ng/mg ($n = 3$).
13. B. W. Zweifach, *Annu. Rev. Physiol.* **35**, 117 (1973).
14. Because ricin binds more avidly to components of the basement membrane (25) than to the endothelial cell surface, it can be used to identify the number and location of sites of exposed basement membrane (26). Perfusion of ricin after fixation helps to eliminate the role of blood flow and pressure.
15. G. Majno, G. E. Palade, G. I. Schoeffl, *J. Biophys. Biochem. Cytol.* **11**, 607 (1961); E. Svensjo and G. J. Grega, *Fed. Proc.* **45**, 89 (1986); D. M. McDonald, *Am. J. Physiol.* **266**, L61 (1994).
16. We found fewer ricin-labeled leaky vessels in double transgenic K14-Ang1/VEGF mice than in K14-VEGF mice after treatment with mustard oil. This difference corresponded to the difference in the amount of

Evans blue leakage. The few leaky sites in inflamed ears of K14-Ang1/VEGF mice were located in small venules and in capillary-like vessels, similar to the location of leaky vessels in K14-VEGF mice.

17. I. Baumgartner et al., *Circulation* **97**, 1114 (1998).
18. D. W. Losordo et al., *Circulation* **98**, 2800 (1998).
19. R. M. Schainfeld and J. M. Isner, *Ann. Intern. Med.* **130**, 442 (1999).
20. R. B. Fick Jr. et al., *J. Appl. Physiol.* **63**, 1147 (1987); P. J. Barnes, *J. Allergy Clin. Immunol.* **83**, 1013 (1989); J. S. Erjefalt et al., *Clin. Exp. Allergy* **28**, 1013 (1998); T. Ohru et al., *J. Allergy Clin. Immunol.* **89**, 933 (1992).
21. J. Cunha-Vaz, *Eur. J. Ophthalmol.* **8**, 127 (1998); I. A. Shiels et al., *Med. Hypotheses* **50**, 113 (1998).
22. S. Mesiano, N. Ferrara, R. B. Jaffe, *Am. J. Pathol.* **153**, 1249 (1998).

23. G. Thurston, P. J. Murphy, P. Baluk, J. R. Lindsey, D. M. McDonald, *Am. J. Pathol.* **153**, 1099 (1998).
24. R. K. Bergman and J. J. Munoz, *J. Allergy Clin. Immunol.* **55**, 378 (1975).
25. J. D. Wadsworth, A. Okuno, P. N. Strong, *Biochem. J.* **295**, 537 (1993).
26. G. Thurston, P. Baluk, A. Hirata, D. M. McDonald, *Am. J. Physiol.* **271**, H2547 (1996).
27. P. Baluk, G. Thurston, T. J. Murphy, N. W. Bunnett, D. M. McDonald, *Br. J. Pharmacol.* **126**, 522 (1999).
28. Supported in part by NIH grants HL-59157 and HL-24136. We thank P. Baluk and J. W. McLean for helpful discussions; M. Simmons, T. Murphy, and N. Glazer for technical assistance; and C. Murphy and E. Burrows for help with graphics.

8 July 1999; accepted 8 November 1999

Reduced MAP Kinase Phosphatase-1 Degradation After p42/p44^{MAPK}-Dependent Phosphorylation

Jean-Marc Brondello,* Jacques Pouyssegur, Fergus R. McKenzie†

The mitogen-activated protein (MAP) kinase cascade is inactivated at the level of MAP kinase by members of the MAP kinase phosphatase (MKP) family, including MKP-1. MKP-1 was a labile protein in CCL39 hamster fibroblasts; its degradation was attenuated by inhibitors of the ubiquitin-directed proteasome complex. MKP-1 was a target *in vivo* and *in vitro* for p42^{MAPK} or p44^{MAPK}, which phosphorylates MKP-1 on two carboxyl-terminal serine residues, Serine 359 and Serine 364. This phosphorylation did not modify MKP-1's intrinsic ability to dephosphorylate p44^{MAPK} but led to stabilization of the protein. These results illustrate the importance of regulated protein degradation in the control of mitogenic signaling.

The control of cell division in response to mitogens is mediated at least in part by MAP kinase (MAPK) signaling pathways (1). The p42^{MAPK} and p44^{MAPK} enzymes [extracellular signal-regulated kinase (ERK)-2 and ERK-1] are activated in cells stimulated with mitogens, by phosphorylation on threonine and tyrosine residues within protein kinase subdomain VIII, mediated by a class of MAP kinase (or ERK) kinases typified by MEK1 (2). Inhibition of p42^{MAPK} and p44^{MAPK} blocks cell-cycle reentry (3) and is principally mediated *in vivo* by members of a family of dual specificity phosphatases, of which MAP kinase phosphatase (MKP-1, also called 3CH134, CL100, or erp) is archetypal (4, 5). At least nine distinct MKP family members have been cloned, most, if not all, of which are the products of immediate early

genes and therefore under tight transcriptional control (5, 6). MKP-1, MKP-2, and MKP-3 are transiently synthesized after activation of p42^{MAPK} and p44^{MAPK}, suggesting the presence of a negative feedback loop to regulate p42^{MAPK} and p44^{MAPK} (5-7). To determine whether expression of the MKP-1 protein is also subject to control, we determined the half-life of MKP-1 in CCL39 fibroblast cells (Fig. 1A). MKP-1 was barely detectable in quiescent CCL39 fibroblasts, but its expression level was increased in cells stimulated with mitogens before [³⁵S]methionine labeling and immunoprecipitation (8). Its half-life was on the order of 45 min.

Because many labile proteins are targeted for degradation by the ubiquitin-directed proteasome complex (9), we analyzed the effects of a proteasome inhibitor *N*-acetyl-leu-leu-norleucinal (LLnL) (10) and a lysosomal cysteine protease inhibitor, *N*-[*N*-(L-3-trans-carboxiraine-2-carbonyl)-L-leucyl]-agmatine (E64) (10) on MKP-1 degradation (Fig. 1B). After treatment of cells with serum to induce synthesis of MKP-1 and blockade of further protein synthesis by cycloheximide, the amount of MKP-1 decreased at a similar rate in control cells and

Institute of Signaling, Developmental Biology and Cancer Research, CNRS UMR 6543, Centre A. Lacasagne, 33 Avenue de Valombrose, Nice 06189, France.

*Present address: The Scripps Research Institute, Department of Molecular Biology, MB-3, 10550 North Torrey Pines Road, La Jolla, CA 92037, USA.

†To whom correspondence should be addressed. E-mail: mckenzie@unice.fr

LINKED CITATIONS

- Page 1 of 1 -



You have printed the following article:

Leakage-Resistant Blood Vessels in Mice Transgenically Overexpressing Angiopoietin-1

G. Thurston; C. Suri; K. Smith; J. McClain; T. N. Sato; G. D. Yancopoulos; D. M. McDonald
Science, New Series, Vol. 286, No. 5449. (Dec. 24, 1999), pp. 2511-2514.

Stable URL:

<http://links.jstor.org/sici?sici=0036-8075%2819991224%293%3A286%3A5449%3C2511%3ALBVIMT%3E2.0.CO%3B2-M>

This article references the following linked citations:

References and Notes

¹ **Signaling Vascular Morphogenesis and Maintenance**

Douglas Hanahan

Science, New Series, Vol. 277, No. 5322. (Jul. 4, 1997), pp. 48-50.

Stable URL:

<http://links.jstor.org/sici?sici=0036-8075%2819970704%293%3A277%3A5322%3C48%3ASVMAM%3E2.0.CO%3B2-S>

¹ **Angiopoietin-2, a Natural Antagonist for Tie2 that Disrupts In vivo Angiogenesis**

Peter C. Maisonpierre; Chitra Suri; Pamela F. Jones; Sona Bartunkova; Stanley J. Wiegand; Czeslaw Radziejewski; Debra Compton; Joyce McClain; Thomas H. Aldrich; Nick Papadopoulos; Thomas J. Daly; Samuel Davis; Thomas N. Sato; George D. Yancopoulos

Science, New Series, Vol. 277, No. 5322. (Jul. 4, 1997), pp. 55-60.

Stable URL:

<http://links.jstor.org/sici?sici=0036-8075%2819970704%293%3A277%3A5322%3C55%3AAANAFT%3E2.0.CO%3B2-U>

² **Increased Vascularization in Mice Overexpressing Angiopoietin-1**

Chitra Suri; Joyce McClain; Gavin Thurston; Donald M. McDonald; Hao Zhou; Eben H. Oldmixon; Thomas N. Sato; George D. Yancopoulos

Science, New Series, Vol. 282, No. 5388. (Oct. 16, 1998), pp. 468-471.

Stable URL:

<http://links.jstor.org/sici?sici=0036-8075%2819981016%293%3A282%3A5388%3C468%3AIVIMOA%3E2.0.CO%3B2-%23>

NOTE: The reference numbering from the original has been maintained in this citation list.